

# Chain Noise Excitation in Combustion Engines – Numerical Simulation and Verification of Different Chain Types

**T. Schaffner, M. Sopouch, H.H. Priebisch**

Christian Doppler Lab of Engine and Vehicle Acoustics,  
Inst. for Combustion Engines, TU Graz, Austria and  
AVL List GmbH, Graz, Austria  
email: [hans-herwig.priebisch@accgraz.com](mailto:hans-herwig.priebisch@accgraz.com)

## Abstract

Synchronous belts and chains are the main competitors for timing drives of passenger car engines. The expected lifetime of today's cars and the downward drift of consumer acceptance for longer service down time leads to a renaissance of chains. However, chain drives can noticeably contribute to the interior noise, which has to meet the demand of discerning consumers.

This paper presents a comprehensive multi-body dynamics (MBD) model, which takes into account the entire timing drive as a fully coupled system. After a short summary of the theory, two chain systems (bushing chain and silent chain) are compared by simulated and verified results for the timing drive of a gasoline engine. In the second part the potential of excitation reduction by a novel chain system (SmartChain B.V.) in comparison to the bushing chain and silent chain is shown for a two sprocket drive.

## 1 Introduction

For passenger car engines, natural frequencies (1<sup>st</sup> mode) of timing chain drives are typically in the range between 80 and 250 Hz. The corresponding natural modes usually show rotational oscillations of the camshaft(s) against the crankshaft. The chain spans act like elastic connections between the sprockets.

In addition to the low-frequency dynamics determined by the engine orders, high frequency oscillations occur. They are caused by polygon effects or meshing impacts [1] (when chain links get into contact with sprockets) and correspond to the meshing frequency. This causes a narrow band excitation of the structure audible as a speed dependent whine noise. The high-frequency excitation is typically transferred to the engine at support positions of shafts, sprockets, guides and at the tensioner.

This noise can be clearly recognized in the passenger compartment if the meshing frequency corresponds to a natural frequency of the engine structure. Figure 1 shows the Campbell-diagram of the average interior sound pressure in a recent car compartment. The "chain line" at the polygon order is obviously present and the whine noise was clearly audible by the passengers. The numerical simulation of the excitation mechanism requires detailed models of chain and chain tensioner [1]. Additionally the interaction between sub-systems (e.g. chain drive and camshaft) must be considered by modeling the entire timing drive [7]. Thus, camshafts as well as all driven valve trains are modeled and regarded as members of the entire MBD representation. The resulting fully coupled model of the timing drive is a key point for correct reproduction of chain-drive/camshaft interactions.

Figure 2 gives an overview about the timing drive system as it is considered in the model. The software package AVL-TYCON is used to perform the simulation.

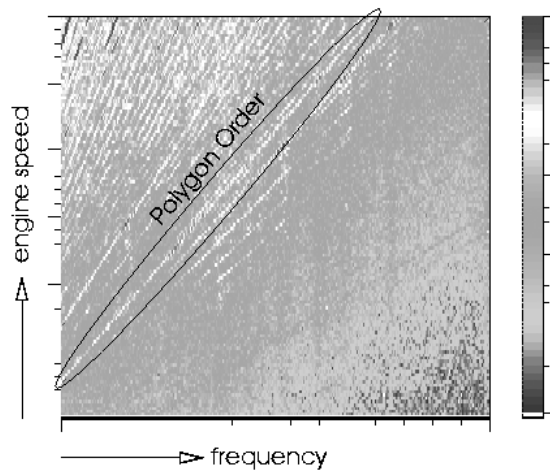


**Figure 1: Average Interior Sound Pressure**

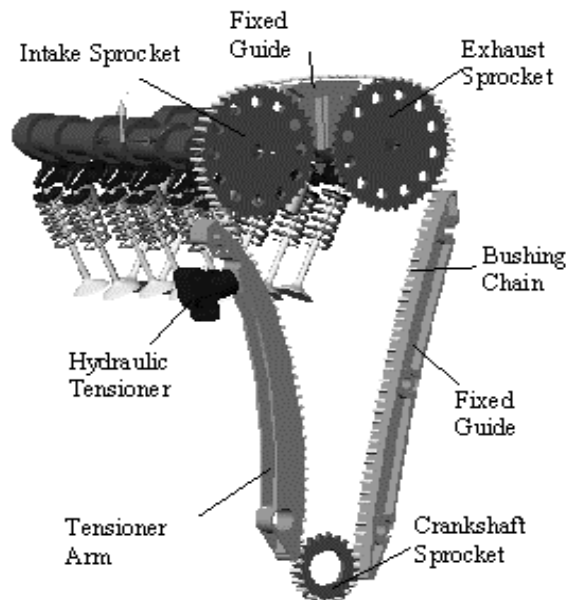


**Figure 2: Relevant Elements of the Timing Drive**

## 1.1 Boundary conditions

The chain system is cut out of the engine and the following boundary conditions are set:

- Mechanical connections to the engine block and cylinder head

Several parts of the chain system are connected to the engine block and the cylinder head: valves, valve springs, hydraulic lifters, camshafts to head; guides and hydraulic tensioner to block. Hereby block/head are assumed to be rigid and fixed inertially. Combinations of linear springs and dampers are used to model the flexibility as well as the dissipation behaviour of interfaces listed above.

- Crankshaft

The crankshaft sprocket is assumed to be radially fixed in space. The rotational movement of the sprocket is applied by a kinematic boundary condition. This implicates the neglect of the interaction between chain drive and crankshaft which is a reasonable assumption due to the big inertia of the crankshaft..

- Valves

Beside the mechanical connections the valves have interfaces to the combustion gases. These are considered by kinetic boundary conditions (forces on the valve faces).

- Hydraulic tensioner and hydraulic lifters

Non mechanical interfaces of the tensioner and the hydraulic lifters are the hydraulic connections to the oil circuit of the engine and the surrounding. The connection to the oil circuit is considered by a constant oil pressure as a function of average engine speed. At the connection to the surrounding a constant pressure is assumed.

## 2 Basic equations

The modelling methodology splits all elastic structures into rigid bodies and elastic connections between them and sets up the equation of motion for rigid bodies.

Additionally to the equation of motion for the mechanical parts, a hydraulic network is set up for the hydraulic volumes and flow-connections. Furthermore the interaction between the network and the mechanic parts has to be considered.

### 2.1 Rigid bodies and elastic contacts

The simulation of body motion and contacts between chain, sprockets and guides is based on the following equations:

#### 2.1.1 Rigid body equation

For rigid bodies equation (1) is used

$$\mathbf{M}_{comp} \cdot \ddot{\mathbf{q}}_{comp} = \mathbf{f}_{comp}^{(a)} + \mathbf{f}_{comp}^* \quad (1)$$

where  $\mathbf{M}_{comp}$  is the matrix of masses and moments of inertia for a specific component,  $\ddot{\mathbf{q}}_{comp}$  denotes the six degrees of freedom of the rigid body accelerations with reference to the component's centre of gravity. The right hand side of the equation contains external loads  $\mathbf{f}_{comp}^{(a)}$  and joint forces and moments  $\mathbf{f}_{comp}^*$ . External loads (e.g. gas force) and moments are functions given in time, that are determined from given measurement data. The non-linear terms of excitation loads in contacts are given by joints equations, connecting one body to another (e.g. chain's bush to sprocket).

Applying the simplifications:

- Principle axis of inertia agree with the axis of the local (body fixed) co-ordinate system: the matrix of masses becomes diagonal ( $\mathbf{M}_{comp} = \text{diag}(\mathbf{M}_{comp})$ ).
- Rotational motion components related to local co-ordinate system (Eulerian approach): time invariance of inertia tensor ( $\mathbf{M}_{comp} = \text{const.}$ )

as well as the extension to a system of rigid components (the number of components is  $n_{comp}$ )

$$\mathbf{M}_{system} \cdot \ddot{\mathbf{q}}_{system} = \mathbf{f}_{system}^{(a)} + \mathbf{f}_{system}^* \quad (2)$$

leads to a ODE-system where the coupling is only present on the right hand side. Hence, accelerations  $\ddot{q}_{system,i}$  of each generalised co-ordinate can be expressed by a simple scalar equation:

$$\ddot{q}_{system,i} = \frac{f_{system,i}^{(a)} + f_{system,i}^*}{M_{system,i}} \quad (3)$$

where  $M_{system,i}$  denotes engine components masses or moments of inertia respectively.  $i$  ( $1 \leq i \leq 6 \cdot n_{comp}$ ) is the index of the main diagonal element of  $M_{system}$  as well as of the corresponding force-vector-component.

The integration of (3) is performed in time domain using e.g. a predictor/corrector method where the deviation between predictor (explicit) and corrector (implicit) is utilised for an automatic step size control. Due to the high non-linearity of the investigated systems, a root finder algorithm to detect state events (e.g. impacts and separations in contacts) is applied.

### 2.1.2 Contact of solids equation (elastic foundation model)

The determination of contact forces  $f_{comp}^*$  based on profile's interference of two solids (rigid bodies) usually requires the solution of an integral equation for the pressure, [9]. Taking into account the huge amount of contact pairs which arise in the timing drive domain (e.g. contact of chain to sprockets and guides) there is a strong request for a simplified contact approach. Thus, a simple Winkler elastic foundation ("mattress") is used.

The representation of the profile's shape is done by means of bezier-splines (restricted to plane contours) or an arc&line based profile decomposition. For further details see [3].

## 2.2 Hydraulic

The hydraulic volumes and flow connections are modeled as a hydraulic network. Volumes are treated as hydraulic capacities and the connections between the volumes are regarded as hydraulic resistances. Mass forces due to the hydraulic medium are neglected, which means that no hydraulic inductivities appear. The connection between mechanic and hydraulic is realized via plunger elements.

### 2.2.1 Hydraulic Capacities

For each hydraulic capacity the following equation is solved in time domain to calculate the pressure in the volume:

$$V \cdot \dot{p} = \beta(p) \cdot \sum \dot{V} \quad (4)$$

$V$  is the actual chamber volume,  $\dot{p}$  is the pressure change in the volume,  $\beta$  denotes the pressure dependent bulks module of the medium and  $\sum \dot{V}$  is the sum of the flows into and out of the volume.

### 2.2.2 Hydraulic Resistances

For hydraulic resistances it is assumed that they come under one of the following three types. Hereby, volume flows can be calculated by the stated equation.

**Lines:**

$$\dot{V} = \text{sign}(\Delta p) \cdot \frac{2|\Delta p|}{\sqrt{(\lambda \frac{l}{d} + \sum \zeta) \cdot \rho}} \cdot A \quad (5)$$

In this equation the symbols denotes the following physical quantities:

- $\Delta p$  ...pressure difference across the resistance
- $l$  ...length of the line
- $d$  ...hydraulic diameter of the line
- $\lambda$  ...friction number
- $\rho$  ...density of the medium
- $\sum \zeta$  ...sum of the additional resistances
- $A$  ...cross-sectional area of the line
- $\dot{V}$  ...volumetric flow.

The friction number is determined from the Colbrook-Nikuradse diagram (see [4]).

**Orifice, Throttle and Valve:**

$$\dot{V} = \text{sign}(\Delta p) \cdot \sqrt{\frac{2|\Delta p|}{(1 + \zeta) \cdot \rho}} \cdot A \quad (6)$$

$\zeta$  denotes the Reynold's-Number dependent flow resistance.  $A$  can be dependent on the co-ordinate of a mechanical element (e.g. in the case of a throttle or valve).

**Leakage:**

For leakages volume flow is derived under the assumptions of laminar flow and flow only in the direction of the leakage.

$$\dot{V} = \frac{h^2}{12l\eta} \cdot \Delta p \cdot (w \cdot h) \quad (7)$$

- $h$  ...height of the leakage
- $w$  ...width of the leakage
- $l$  ...length of the leakage
- $\eta$  ...dynamic viscosity of the medium

**2.2.3 Coupling Mechanic and Hydraulic**

The mechanical and hydraulic domains are connected via plunger elements, which couple hydraulic capacities and mechanic bodies. The force  $f^*$  onto the mechanical element caused by the hydraulic capacity under pressure  $p$  is calculated by

$$f^* = p \cdot A \quad (8).$$

Herein,  $A$  denotes the cross-sectional area of the plunger. For the hydraulic capacity the coupling means a variable chamber volume  $V$ , which depends on the position of the coupled mechanical body.

**3 Simulation Methodology**

**3.1 Chains**

To simulate longitudinal/transversal vibrations and polygon-effect, a discrete 2D-model is applied. Each chain-link is considered as a rigid body with three DoF's in its plane of motion. The chain's

elastic/viscous behavior (incl. clearance) and friction in the joints is taken into account by force- units between the links.

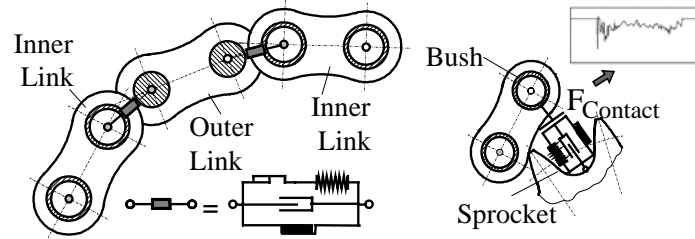


**Figure 3: MBD representation of bushing chain and contact to sprocket**

Contact elements serve to consider the interaction between chain-links and sprockets/guides. The exact profiles at sprockets/guides and links are considered, which is an absolute necessity when predicting meshing impacts (Figure 3). The differences between bushing- and silent-chain are the profiles and the characteristics of the stiffness in the connection between the link-rows (Figure 4).

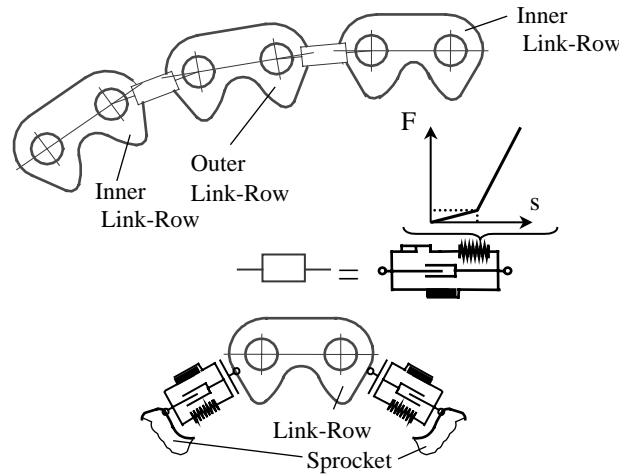


**Figure 4: MBD representation of silent chain and contact to sprocket**

### 3.2 Hydraulic Tensioner

The tensioner is one of the most important elements with regard to the chain drive's dynamic behavior, [8]. A detailed combined hydraulic/mechanic-model is applied. In addition, the following specific effects are to be considered:

- Feed due to supply pressure and retainer spring
- Damping due to oil flow through orifice between supply and working room
- Damping due to leakage gap between plunger and housing
- Compressibility of oil in working room

### 3.3 Camshafts & Valve Trains

Torsional and bending behavior of the camshafts is taken into consideration by a discrete model consisting of a series of 6 DoF rigid bodies connected with massless beam-elements. For the camshaft bearings an impedance method is used to introduce the non-linear characteristics of the oil gap.

The MBD-Model for the valve trains contains all relevant parts like follower, hydraulic-lifter, valve (incl. valve seat) and valve spring. For the hydro-lifter a hydraulic model is applied. For further details see [5].

## 4 Primary Dynamics

The correct reproduction of the chain drive's primary dynamics is an absolute necessity when predicting structural excitations.

Excitation of the system arise mainly from three sources. The first source of excitation are the periodical speed fluctuations of the crankshaft sprocket due to the mass forces inside the crank trains of the engine and due to the combustion process. The second source is the excitation of the system due to force fluctuations at the each cam and therewith periodical torque fluctuations at the camshaft sprockets. These force fluctuations are caused by the valve spring forces, the mass forces of the valve train components and the pressure-forces from the gas inside the combustion chamber and the ducts. The third source is the polygon effect of the chain drive, a "inner" excitation. The polygonal wrap of sprockets/guides by the chain causes a periodic fluctuation of the effective radius during sprocket's rotation, which leads to an excitation of longitudinal and transversal vibrations of the connected spans. Furthermore, the relative velocity measured in the contact direction between the chain's bush or link and sprocket's mesh leads to impacts, which occur periodically. These effects appear with meshing frequency of the drive and are well known as the "polygon effect", see [1]. Additionally, a half polygon order can be generated due to different lengths of the outer and inner links or link rows of the chain. Both chain types, bushing chain and silent chain, do have these differences. The bushing chain drive does not generate a half polygon order because the gaps of the sprockets are quite wide and the point of first contact during engaging is close to the ground of the profile where the contact angle is almost  $180^\circ$ , see Figure 5. As a consequence different lengths do not lead to a temporal shift of the impact event. In contrast, at the silent chain the link plate's teeth are more enclosed by the sprocket's profile and the contact angle is approximately  $60^\circ$ . Hence, the point of first contact at the sprocket is either closer to the addendum circle (and therewith earlier) or closer to the dedendum circle (and therewith later). The different lengths also leads to a different radial position of inner and outer link rows. Therefore, this differences generate significant speed fluctuation in half the polygon order.

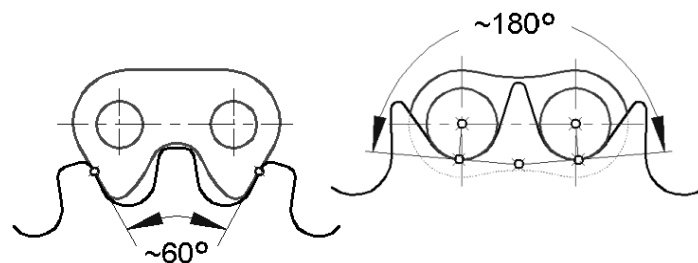


**Figure 5: Contact Angle of Bushing Chain and Silent Chain**

### 4.1 Primary Dynamics: Bushing Chain

As a first example the validation of the primary dynamics of a bushing chain timing drive applied to a recent 3 cylinder DOHC gasoline engine is shown, Figure 2. The chain drive is equipped with a 8 mm bushing chain (130 links) the number of teeth at the crankshaft sprocket is 20. An automatic hydraulic chain tensioner combined with a tensioner arm is utilized to provide the required pre-tension. In contrast to usual tensioners, it does not contain a check valve between oil supply and working volume. Discharge and refilling of the working volume is done via an orifice which leads to a quit "soft" behavior of the tensioner. The tensioner behaviour was validated first in a separate test in order to adjust the model parameters [6]. Since, chain-drive induced noise dominates at idle, where the noise excitation due to combustion is of minor importance, investigation results are shown for idle operating conditions.

The critical speed of this engine was found at 3400 rpm. At this speed the 1<sup>st</sup> natural frequency of the chain drive (about 85 Hz) corresponds with the 1.5<sup>th</sup> engine order excitation. The natural frequency is

rather low and mainly affected by the soft tensioner. The correlation in order domain is given in Figure 6. Both, the engine main orders 1.5<sup>th</sup>, 3<sup>rd</sup>, 4.5<sup>th</sup> and the polygon order (20<sup>th</sup>) agree reasonably with the measurements. At 4000 and 4500 rpm the simulation show a amplification of the 6<sup>th</sup>, 7.5<sup>th</sup> and 9<sup>th</sup> order due to a natural frequency at 560 Hz. This resonance can not be seen that clearly in the measurement. The gray spot indicates the influence of the rotational-velocity transducer-set with a natural frequency of 1365 Hz, which is excited by the polygon order. This behavior can also be seen in the calculation, as the transducer-set is part of the model. For further details concerning the primary dynamics of the bushing chain drive see [5].

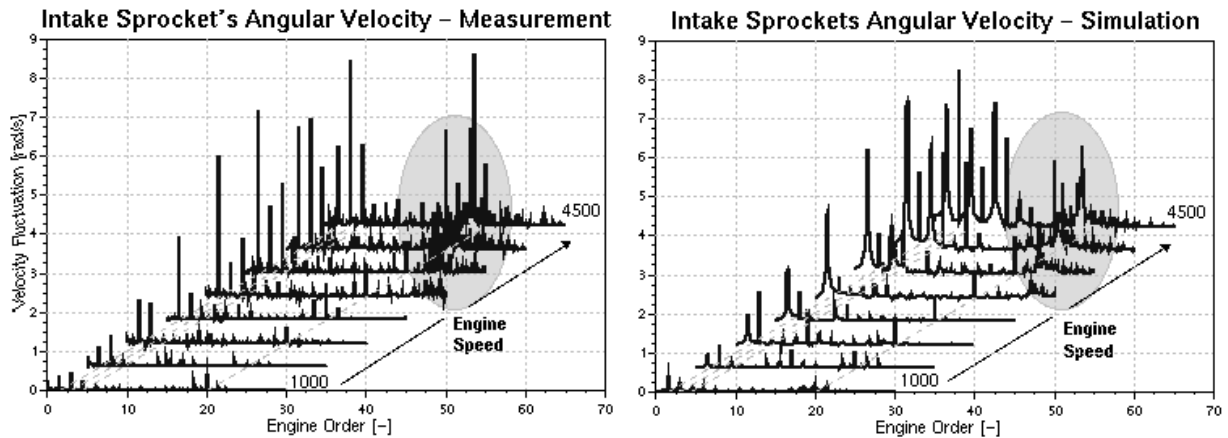


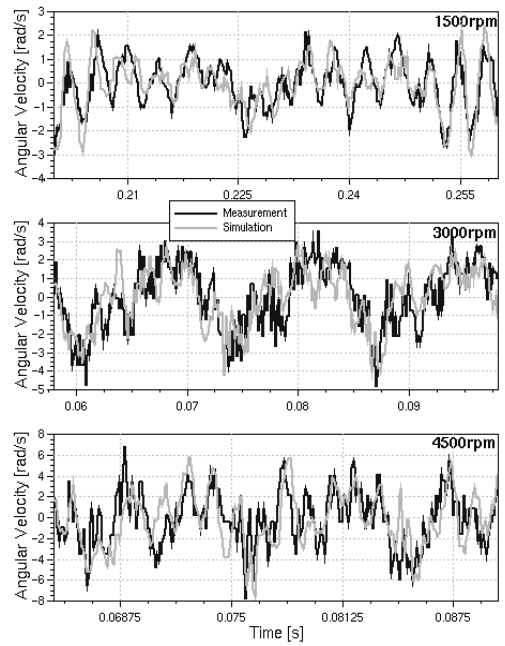
**Figure 6: Comparison of calculated and measured angular velocities of the intake camshaft front (bushing chain)**

## 4.2 Primary Dynamics: Silent Chain

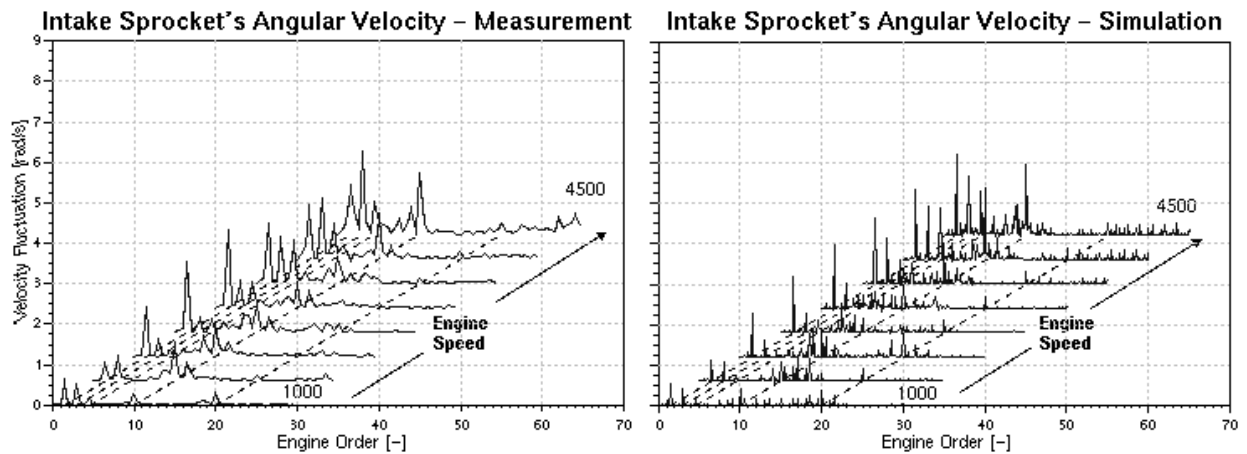
The second example is a silent chain drive. The drive is applied to the same engine as the bushing chain in first example to enable direct comparison of both chain types. Additionally, the following changes had to be made: the fixed guide between the camshaft sprockets was omitted and the stiffness of the rotational transducer clutches was increased significantly to avoid resonances with the polygon order in the viewed speed range. Concerning pitch and length the silent chain is identical with the bushing chain, but its weight is approximately 10% higher. The combination of more weight with the different stiffness characteristic leads to a first natural frequency of the chain drive at 70 Hz. Compared to the bushing chain drive, the automatic chain tensioner of the silent chain shows a higher flow resistance for refilling and discharging. This was the result of a test bench setup somewhat different to the bushing chain version.

Figure 7 compares the simulated fluctuation of the intake sprocket's angular velocity with measurements in time domain at three speeds. In general, it can be seen that the correlation between simulation and measurement is good for all three speeds shown. The correlation in order domain is given in Figure 8. Both, the engine main orders 1.5<sup>th</sup>, 3<sup>rd</sup>, 4.5<sup>th</sup>, the polygon order (20<sup>th</sup>) and the half polygon order (10<sup>th</sup>) agree good with the measurements.

Figure 9 gives a closer view into Figure 8 by viewing along the lines for the 10<sup>th</sup> and the 20<sup>th</sup> order. The calculated curves agree reasonably with the measurement. Big differences for both orders can be seen around 670 Hz due to an natural frequency in the model which is not present in the experiment.



**Figure 7: Comparison of simulated intake camshaft rotation with measurement in time domain (silent chain)**



**Figure 8: Comparison of simulated intake camshaft rotation with measurements in order domain (silent chain)**

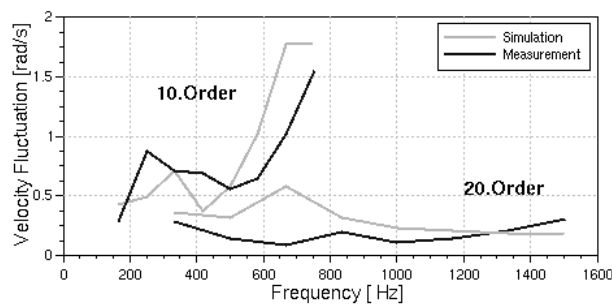


**Figure 9: Comparison of simulated intake camshaft rotation with measurement in frequency domain for the 10<sup>th</sup> and 20<sup>th</sup> order (silent chain)**

### 4.3 Primary Dynamics: Bushing versus Silent Chain

In general the values of the velocity fluctuations for the silent chain are significantly smaller than for the bushing chain (approximately by a factor of 0.5, see Figure 6 and Figure 8). More detailed investigations based on simulation have been shown that this reduction is mainly caused by the stiffer tensioner of the silent chain drive. The change of the chain type itself contributes to a small extent only.

Figure 10 shows the comparison of the simulated angular velocity fluctuations at the intake camshaft sprocket for the 10<sup>th</sup> and 20<sup>th</sup> order. To avoid possible misinterpretation caused by rotational transducer-set resonance arising with the bushing chain drive, the rotational movement of the sprockets are compared instead of the transducer's ones.

All four curves in Figure 10 show peaks at 670 Hz which is an eigenfrequency of the models.

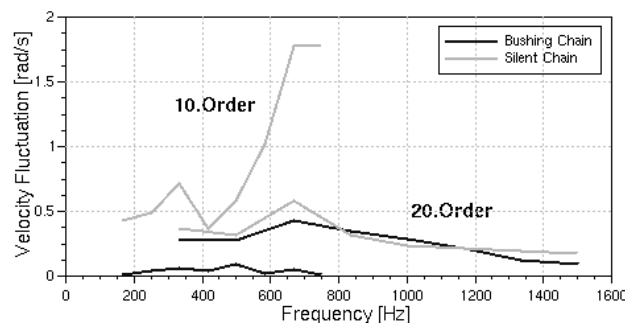


**Figure 10: Comparison of the simulated velocity fluctuations of the intake sprocket for Bushing Chain and Silent Chain**

10<sup>th</sup> order: The bushing chain shows almost no fluctuations, whereas the silent chain generates the highest fluctuations in this order. An explanation is given in chapter 4.

20<sup>th</sup> order: The differences between the two chain types are surprisingly small, the actual design of the silent chain drive seems not exploit the full potential of this chain concept.

## 5 Structural Excitation

Structural excitation was investigated for the same two configurations as under chapter 4.

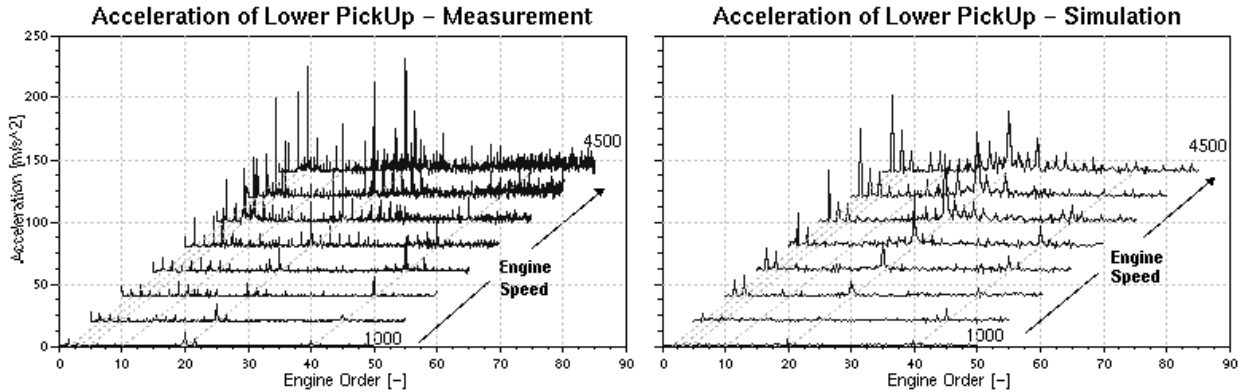
For the assessment of the structural excitation, forces arising in the interfaces (joints) between chain-drive and engine structure have been examined: Bearing forces of crankshaft and camshafts, supporting forces of tensioner arm and guide mounts and tensioner pressure, see [5]. These forces can be understood as excitations transferred to the engine block and represent a relative measure for the structure borne noise excitation.

Various experimental as well as numerical investigations proved that an essential share of whine noise excitations (half polygon order, polygon order and their harmonics) are transferred via the tensioner arm mount. Because mounting forces are difficult to measure, acceleration pick-ups have been applied on the arm at three locations to quantify the structure borne noise excitation. The pick-ups are placed close to the tensioner, in the middle of the arm and close to the arm mount.

Mainly the latter has been used for the verification of structural excitation.

## 5.1 Structural Excitation: Bushing Chain

Figure 11 shows the results for simulation and measurement of the accelerations close to the tensioner arm mount. The spectra of the acceleration fluctuations are given for the entire speed range. The correlation between measurement and simulation is acceptable. The main engine orders (1.5<sup>th</sup>, 3<sup>rd</sup>, 4.5<sup>th</sup>) and polygon order (20<sup>th</sup>) as well as their 1<sup>st</sup> harmonic (40<sup>th</sup>) can be observed clearly in the order-traces in Figure 11. In particular at medium engine speeds the polygon order is already one of the dominating frequencies.



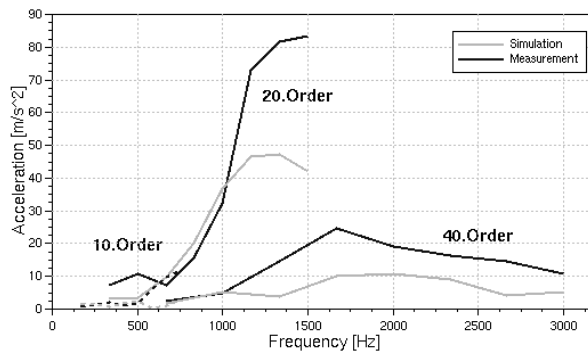
**Figure 11: Comparison of simulated and measured accelerations near tensioner arm mount (bushing chain)**

Figure 12 giving a view into Figure 11 along the relevant order lines for whine noise excitation (10<sup>th</sup>, 20<sup>th</sup> and 40<sup>th</sup> engine order), can be commented as follows:

10<sup>th</sup> order (dotted line): Almost no contribution can be seen in this order, as it is expected for the bushing chain.

20<sup>th</sup> order: The simulation shows the same characteristic as the measurement. In the lower frequency range (corresponding to the lower engine speed range) the simulation meets the measurement very good, but in upper frequency range (corresponding to upper speed range) the simulation shows a significantly lower contribution.

40<sup>th</sup> order: The picture is almost the same as with the 20<sup>th</sup> order. In the lower frequency range the simulation meets the measurement very good, but in the upper frequency range the simulated accelerations are approximately by a factor 2 smaller than the measured ones.



**Figure 12: Comparison of simulated arm mount acceleration with measurement for the 10<sup>th</sup>, 20<sup>th</sup> and 40<sup>th</sup> engine order (bushing chain)**

## 5.2 Structural Excitation: Silent Chain

The structural excitation of the silent chain is observed in the same way as for the bushing chain. The only difference is that the 30<sup>th</sup> order (3<sup>rd</sup> harmonic of the half polygon order), is viewed additionally, as it appears clearly.

Figure 13 shows the comparison of the accelerations close to the tensioner arm mount for the entire speed range. Figure 14 again shows details of the comparison along the 10<sup>th</sup>, 20<sup>th</sup>, 30<sup>th</sup> and 40<sup>th</sup> order lines.

10<sup>th</sup> order: In the lower frequency range the simulation has the same shape as the measurement, especially the resonance peak around 320 Hz can be clearly seen in the simulation, too. Unfortunately the amplitudes are much smaller in the simulation. In upper frequency range the simulation is on the same level of amplitudes as the measurements, but does not show the resonance peak of the measurement at 670 Hz.

20<sup>th</sup> order: The measurement shows two resonance peaks, the first one at 670 Hz and the second one at 1350 Hz. The simulation does only show the first peak at 670 Hz, but with much smaller magnification. Additionally, the simulation indicates a resonance around 1150 Hz, which can not be seen in the measurement. Apart from the magnification at 1150 Hz the simulated acceleration amplitudes are significantly smaller than the measured ones.

30<sup>th</sup> order: The simulation meets the measurement very well, even the resonance peak at 1500 Hz can be observed with the same amplitude in both simulation and test.

40<sup>th</sup> order: Up to the 1000 Hz the simulation meets the measurement, but above this limit the simulation result is much smaller than the measured one. Additionally, the resonance peak at 1350 Hz can not be seen in the simulation and the magnification starting with 2350 Hz is too small in the simulation.

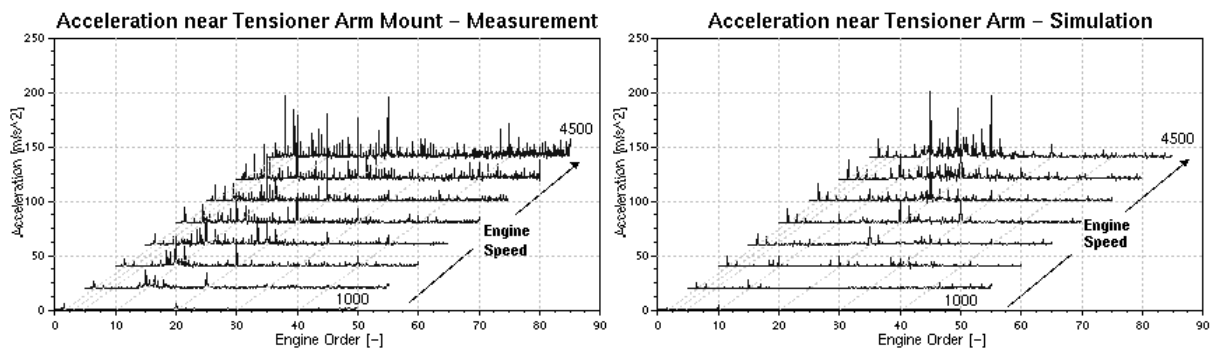


**Figure 13: Comparison of calculated and measured accelerations near tensioner arm mount (silent chain)**

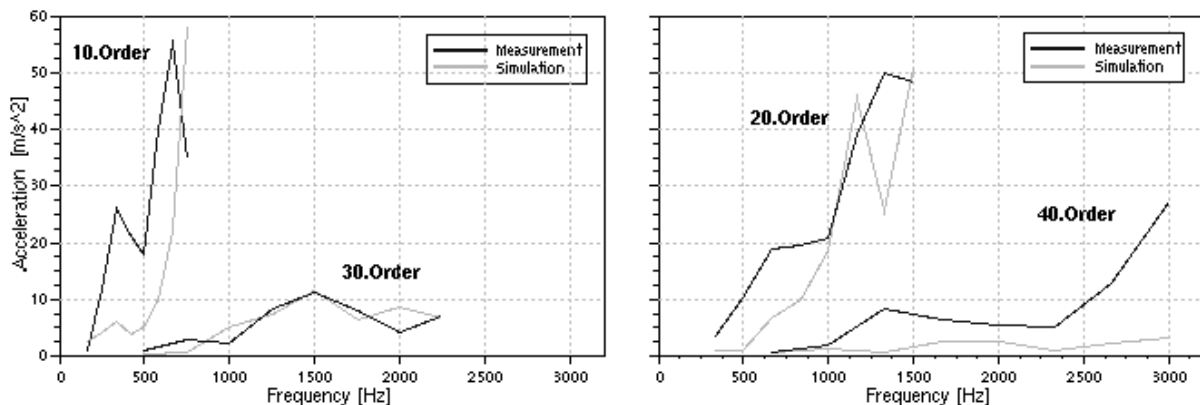


**Figure 14: Comparison of simulated arm mount acceleration with measurement for the 10<sup>th</sup>, 20<sup>th</sup>, 30<sup>th</sup> and 40<sup>th</sup> engine order (silent chain)**

### 5.3 Structural Excitation: Bushing versus Silent

Figure 15 shows the comparison of simulated acceleration of the lower pick-up in the 10<sup>th</sup> and 20<sup>th</sup> orders for both the bushing and the silent chains.

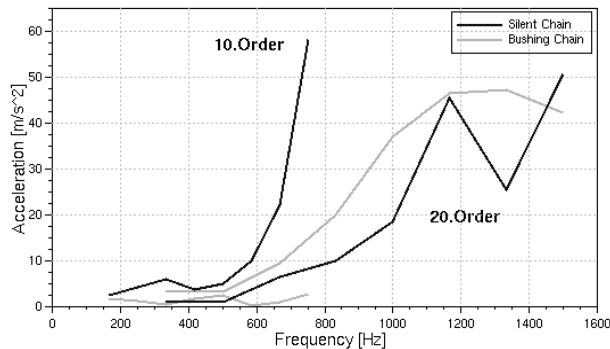


**Figure 15: Comparison of simulated accelerations at tensioner arm mount for Bushing Chain and Silent Chain**

In the 10<sup>th</sup> order the expected behavior can be seen. The contribution of the bushing chain to this order amplitude is very little (see chapter 4). In contrast the silent chain generates strong accelerations, especially in the higher frequency range.

In the 20<sup>th</sup> order the simulated accelerations of bushing chain and silent chain are on the same level. Again, the actual design of the silent chain does not exploit the full potential of the design concept.

## 6 Structural Excitation of three different Chain Systems

In general it is known that silent chains run smoother and do not excite the structure as much as bushing chains, [2]. The potential of the silent chain concept is related to the used profiles for the link rows and sprockets, whereas the profiles of the sprockets of the bushing chain – according to the definition of DIN 8196 – don't play a significant role [6]. In case of a not optimized combination of sprocket profile and link row profile for the silent chain the advantage of the concept can be lost easily, see chapter 4.3 and 5.3.

In the following part it is shown how the chain drive dynamics can be improved by a new chain concept.

### 6.1 Smart Chain Concept

The improvement is realized by guiding the chain in such a way that the centres of the pins of the chain follow a specific theoretical path in the stationary (=fixed) plane. The theoretical path is defined in such a way that for a prescribed constant rotational speed of a sprocket, the velocity of the chain at the straight part of the path is constant, too.

This is enabled by consistent separation of the functions of chain guidance and transmission of the circumferential force. This is achieved by guiding the chain in both in the rotating plane of the sprocket and in the stationary plane. The chain plates, originally consisting of an approximately “eight-shaped” contour, are supplied with two precisely shaped abutments  $n$  at one side of the chain plate. At each side of the sprocket a ring is mounted, which serves as a rotating guide for the abutments. The contours of the abutments have been calculated such that the centres of the pins follow the theoretical path. The chain plate with the abutment works together with the rotating guide ring and functions as a lever. The stationary

guides control the centres of the pins along the straight section. For further details concerning the design see [10].

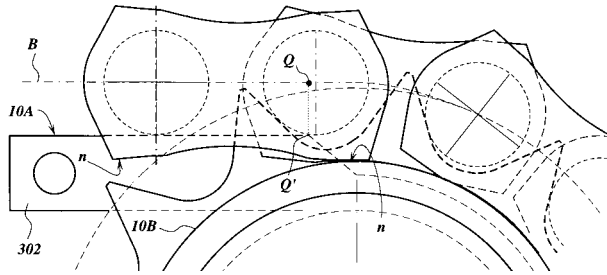


**Figure 16: The novel chain with abutments on both sides and with one design variant for the fixed guide**

## 6.2 Comparison of the Chain Systems

The comparison of the three different chain systems is made for a simple drive with two sprockets (20/40 teeth) and chains with 8mm pitch. Guides were positioned in both free spans. The chain drive does not include a tensioning device in order to prevent adulteration of the specific properties of the various chain types. The initial preload of the chain was created by adjusting the position of the driven sprocket. The driving sprocket (20 teeth) has a constant rotational speed of 3000 rpm and the driven sprocket is loaded by a constant torque of 20 Nm.

Especially in regard to contact mechanics, the new concept shows its major advantage: a continuous, long enduring force build-up occurs between chain and sprocket mesh. **Figure 17** shows the contact forces between the chain link and the driving sprocket in the engagement region. The picture at the left side applies to the new concept. All forces are at a low level (maximum 130 N). Peak forces due to the meshing impacts do not occur.

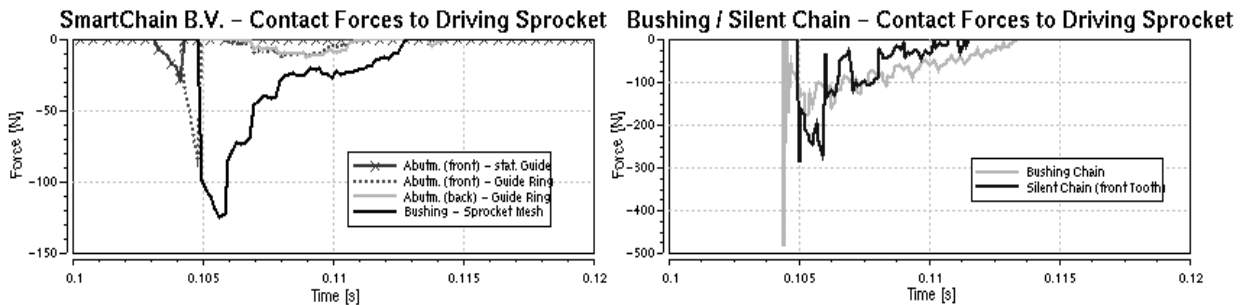


**Figure 17: Dynamic contact forces of the new concept compared to bushing chain and silent chain**

Furthermore, it can be observed that first the abutment at the front side (seen in running direction) makes contact with the stationary guide (—x—). Next, the contact is taken over by the rotating guide (=starting action of lever, .....). As soon as the descending phase is finished, the contact between the bushing and the sprocket mesh follows (——). By the controlled meshing process an acoustically very favourable force transfer occurs, due to the low impulse. As soon as the chain link has wrapped the sprocket totally, the chain link is positioned by the front side and back side abutment of the chain plate which are both supported by the rotating guide. During this process the circumferential force decreases and as a consequence the contact force between bushing and sprocket mesh decreases simultaneously.

In contrast, the picture at the right side of **Figure 17** shows the corresponding courses of the contact forces for bushing chain and silent chain. These chains show the typical force peaks, caused by the meshing impact.

## 7 Conclusion and Outlook

The applications of the outlined modeling theory for two timing drive configurations (bushing chain and silent chain) are shown. The correlation of the results for the primary dynamics in measurement and simulation is very good. The quality of the correlation of the structural excitations is less good, but still sufficient to realize trends and to assess characteristics of different configurations and chain systems.

The simulated results for the novel chain system promises significant reduction of structural excitation in comparison to the bushing chain and the silent chain with single pin joints.

Further improvement of the prediction results for structural excitation can be expected from taking into account the elasticity of the guides (especially the tensioner arm), the interaction to the crankshaft (including interaction to crankshaft and crank train) and introducing the elastic engine block structure with its engine mounts. This is a matter of ongoing work.

## Acknowledgements

This work was funded by the Austrian Government via the Christian Doppler Society. Measurement results were supported by IWIS Ketten, Joh. Winklhofer & Söhne GmbH&CoKG, Germany.

## References

- [1] Fritz P.: *Dynamik schnelllaufender Kettentriebe*, VDI Fortschrittberichte, Serie 11, VDI Bericht 253, VDI Verlag Düsseldorf (1998)
- [2] Baddira G.: *Morse Tec Europe provides to the European Automotive market a significant contribution to noise & emissions reduction, with a new silent chain transmission*, Paper 96EN004, ISATA Conference, (1996)
- [3] Sopouch M., Hellinger W., Pribsch H. H.: *Prediction of vibroacoustic excitation due to the timing chains of reciprocating engines*, Proc. Instn Mech. Engrs Vol.217 Part K: J. Multi-body Dynamics (2003)
- [4] Beitz W., Küttner K.-H. (Editors): *Dubbel – Taschenbuch für den Maschinenbau*, Springer-Verlag, Berlin(1983)
- [5] Sopouch M., Hellinger W., Pribsch H. H.: *Simulation of Engine's Structure Borne Noise Excitation due to the Timing Chain Drive*, Paper 2002-01-0451, SAE Congress, Detroit (2002)
- [6] Sopouch M., Hellinger W., Pribsch H. H., Schaffner T.: *Design Parameters of the Timing Chain Drive and their influence on Structure Borne Noise Excitation*, JSAE, Yokohama (2002)
- [7] Weber C.: *Experimental Investigation into the Dynamic of Engine Timing Chain Behaviour*, SAE Paper 980840, (1998)
- [8] Cuniberti M.: *Analysis and optimisation of a V-engine Chain Timing Drive*, International User Meeting 2003 AVL – Advanced Simulation Technologies, Graz (2003)
- [9] Johnson K. L.: *Contact Mechanics*, Cambridge University Press, Cambridge (1985)
- [10] Korse T., Sopouch M.: *A new Timing Chain with No Cordal Action*, MTZ 5/2004 Volume 65, Vieweg Verlag, Wiesbaden (2004)